

# Spin Hall effect in iron-based superconducting materials: An effect of Dirac point

Sudhakar Pandey<sup>1</sup>, Hiroshi Kontani<sup>1</sup>, Dai S. Hirashima<sup>1</sup>, Ryotaro Arita<sup>2,3</sup>, and Hideo Aoki<sup>4,5</sup>

<sup>1</sup>*Department of Physics, Nagoya University, Furo-cho, Nagoya 464-8602, Japan*

<sup>2</sup>*Department of Applied Physics, University of Tokyo, Hongo, Tokyo 113-8656, Japan*

<sup>3</sup>*PRESTO, Japan Science and Technology Agency (JST), Kawaguchi, Saitama 332-0012, Japan*

<sup>4</sup>*Department of Physics, University of Tokyo, Hongo, Tokyo 113-0033, Japan*

<sup>5</sup>*TRIP(JST), 5 Sanbancho Chiyoda-ku, Tokyo 102-0075, Japan*

We have theoretically explored the intrinsic spin Hall effect in the iron-based superconductor family with a variety of materials. The study is motivated by an observation that, in addition to an appreciable spin-orbit coupling in the Fe 3d states, a character of the band structure in which Dirac cones appear below  $E_F$  may play a crucial role in producing a large spin Hall effect. The theoretical result does indeed predict a substantial spin Hall conductivity in the heavily hole-doped regime such as  $KFe_2As_2$ . The magnitude of the spin Hall effect has turned out to be comparable with that for Pt despite a relatively small spin-orbit coupling, which we identify to come from a huge contribution from the gap opening induced by the spin-orbit coupling at the Dirac point, which can become close to the Fermi energy for the heavy doping.

PACS numbers: 72.25.Ba, 74.25.Jb, 74.70.Xa, 75.47.-m

There is a mounting interest in the spin Hall effect (SHE), where a transverse spin current (as opposed to charge current) is induced in an electric field[1], which provides a most promising way for manipulating spin degrees of freedom for spintronic devices based on nonmagnetic materials. After its theoretical prediction by Hirsch in 1999 [2], which was originally proposed by D'yakonov and Perel' in 1971 [3], investigations were initially focused mostly in semiconductors[4]. More recently, attentions have been extended toward metallic systems [5–17], following experimental reports of a huge spin Hall conductivity (SHC)  $\sim 240\hbar e^{-1}\Omega^{-1}cm^{-1}$  in Pt [5, 6] that is about  $10^4$  times larger than the reported values in semiconductors [4]. A key question then is how we can identify the materials that can exhibit large SHE.

Although SHE is driven by the spin-orbit interaction (SOI), understanding its mechanism in *metallic* systems, especially intrinsic vs extrinsic mechanisms, remains an open issue [1]. While the intrinsic mechanism depends on the details of electronic structure, the extrinsic mechanism is governed by impurities. Here we focus on the former, which has not only successfully accounted for the observed huge SHC in Pt [7, 8, 10, 11], but also predicted a variety of materials, such as several 4d and 5d transition metals [10, 11], as good candidates for SHE. Interestingly, many of these predictions have been realized recently in experiments [16].

In this Letter we explore the possibility of SHE in the recently discovered iron-based superconducting materials, with their variety such as iron pnictides and chalcogenides. While the materials have become a class on its own of high- $T_c$  superconductors after cuprates [18], the reason why we have a fresh look at the materials from the viewpoint of SHE is the following. The iron-based superconductors are typically *multiband* systems, where

various d orbitals are involved in the conduction bands [19]. The bands are entangled (namely, cross with each other), which gives rise to a situation where the orbital character changes as one walks along the Fermi surface. This is realized by an occurrence of “Dirac cones” associated with the band crossing as an interplay between multiorbital character of bands and crystal symmetries [20]. We have also, for the iron compounds, an appreciable spin-orbit coupling (SOC) associated with the Fe 3d states, and a quasi-two-dimensional nature of dispersion. Such features are expected to produce large SHE. For example, Kane and Mele have predicted a large and quantized SHC in graphene when the Dirac cone becomes massive due to an SOI-induced gap at the Dirac point[21]. However, due to extremely small gap due to a weak SOC ( $\simeq 4meV$ )[22] for carbon 2p orbitals, its experimental realization remains challenging. By contrast, a relatively strong atomic SOC of order  $72meV$  [23] for iron 3d orbitals may make the SOC-induced gap at the Dirac points in the iron-based materials large enough for a realization of significant SHE.

This is our reasoning, and, if the Dirac points in these materials lead to a large SHE, then, apart from being a good candidate for spintronics, the materials may also provide an avenue for exploring the Dirac physics in the context of SHE in metallic systems that has recently drawn a surge of interests in case of topological insulators [24]. The present study does indeed predict a substantially large SHC for heavily hole-doped system such as  $KFe_2As_2$ , which is contributed, as expected, by the electronic states in the vicinity of the SOC-induced gap at Dirac points that lie almost at the Fermi level for the heavily doped systems. We stress the Dirac-point-originated large SHE in the iron-based materials is distinct from other systems such as Pt and 4d and 5d tran-

sition metals, where substantially stronger SOC's govern the behavior of SHE.

We consider the realistic band structure of various types of the iron compounds with two Fe atoms per unit cell by incorporating the SOC within an effective tight-binding (TB) Hamiltonian. The Wannier basis of the TB model has been constructed as follows. We first performed a density-functional calculation, where we used the exchange correlation functional proposed by Perdew *et al.* [25], and the augmented plane wave and local orbital (APW+lo) method including the SOC as implemented in the WIEN2k code[26, 27]. We then constructed the TB model using the WIEN2Wannier[28] and the wannier90 [29]. In order to preserve the local symmetry of the Wannier functions, we perform the so-called one-shot Wannierization [30]. Our approach provides a good description of several common electronic features in these materials, such as the pseudogap at the Fermi energy, an effective  $d$ -electron bandwidth of  $4.5 - 5.0$  eV, and the dominant orbital character of electronic states including the local  $d_{xz}/d_{yz}$  degeneracy, etc. These features themselves are almost independent of the SOC, as can be seen in Fig. 1, and expected from the weak SOC for the Fe  $3d$  electrons. However, we shall discuss later that some SOC-induced band features in fact play a crucial role in the SHE.

SHE is investigated with the linear-response theory[31] in the presence of local impurities that give rise to a finite residual resistivity. At  $T = 0$ , SHC consists of two parts,  $\sigma_{xy}^z = \sigma_{xy}^{zI} + \sigma_{xy}^{zII}$ , where

$$\sigma_{xy}^{zI} = \frac{1}{2\pi N} \sum_{\mathbf{k}} \text{Tr} \left[ \hat{J}_x^S \hat{G}^R \hat{J}_y^C \hat{G}^A \right]_{\omega=0} \quad (1)$$

represents the “Fermi-surface term”, while

$$\begin{aligned} \sigma_{xy}^{zII} = & -\frac{1}{4\pi N} \sum_k \int_{-\infty}^0 d\omega \text{Tr} \left[ \hat{J}_x^S \frac{\partial \hat{G}^R}{\partial \omega} \hat{J}_y^C \hat{G}^R \right. \\ & \left. - \hat{J}_x^S \hat{G}^R \hat{J}_y^C \frac{\partial \hat{G}^R}{\partial \omega} - \langle R \leftrightarrow A \rangle \right] \end{aligned} \quad (2)$$

represents the “Fermi-sea term”. Here the charge-current operator is given by  $\hat{J}_\zeta^C = -e\partial\hat{H}/\partial\mathbf{k}_\zeta$  with  $-e(<0)$  being the electronic charge, and  $\zeta = x, y$ , while the  $\sigma_z$ -spin current operator is given by  $\hat{J}_\zeta^S = (-1/e)\{\hat{J}_\zeta^C, \hat{\sigma}_z\}/2$ . The retarded (advanced) Green's function  $\hat{G}^R(\hat{G}^A)$  are given by  $\hat{G}^{R/A}(\mathbf{k}, \omega) = 1/(\omega + \mu - \hat{H} \pm i\hat{\Gamma})$ . Here  $\hat{H}$  is the effective TB Hamiltonian, a  $20 \times 20$  matrix spanned by the two Fe atoms per unit cell in the presence of SOC, and  $\mu$  the chemical potential.  $\hat{\Gamma}$ , the damping due to local impurities, is treated with the T-matrix approximation,  $\hat{\Gamma} = (n_{\text{imp}}/2i)[\hat{T}(-i0) - \hat{T}(+i0)]$ , where  $n_{\text{imp}}$  is the impurity concentration, and  $\hat{T}(\pm i0) = \hat{I}/[1 - \hat{I}\hat{g}(\pm i0)]$ , with  $\hat{g}(\omega) = \sum_{\mathbf{k}} G(\mathbf{k}, \omega)$  representing the T-matrix for a single impurity with an impurity potential  $\hat{I}$ . For simplicity

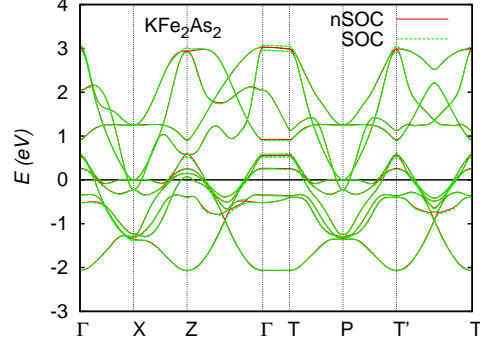


FIG. 1: Band structures with (SOC) and without (nSOC) spin-orbit coupling are shown for  $\text{KFe}_2\text{As}_2$ . The symmetry points are:  $\Gamma = (0, 0, 0)$ ,  $X = (\pi, 0, 0)$ ,  $Z = (\pi, \pi, 0)$ ,  $T = (0, 0, \pi)$ ,  $P = (\pi, 0, \pi)$ , and  $T' = (\pi, \pi, \pi)$ . In our convention, origin of energy is taken to be the chemical potential  $\mu$ , and  $x$ - and  $y$ - are directed along the nearest neighbor Fe atoms.

we consider a constant and orbital-diagonal impurity potential of strength  $I$ , i.e.,  $\hat{I}_{\alpha, \beta} = I\delta_{\alpha, \beta}$ .

In the quantitative investigations that follow, our results for SHC are expressed in unit of  $|e|/2\pi a$ , where  $a$  is the interlayer spacing. For  $a = 6\text{\AA}$ ,  $|e|/2\pi a \sim 645\hbar e^{-1}\Omega^{-1}\text{cm}^{-1}$ . Unless otherwise mentioned, we consider  $I = 6$  eV, and  $n_{\text{imp}} = 0.01$ .

Figure 2 shows the results for SHC for various materials,  $\text{KFe}_2\text{As}_2$ , FeSe, and  $\text{LaFeAsO}_{0.9}\text{F}_{0.1}$ , obtained with the *ab initio* band structures. The dominant contribution is found to arise from the Fermi-surface part, i.e.,  $\sigma_{xy}^z \simeq \sigma_{xy}^{zI}$ , for all the materials considered. We can immediately notice that a large SHC arises in  $\text{KFe}_2\text{As}_2$ , a heavily hole-doped system, while it becomes vanishingly small in undoped FeSe and weakly electron-doped  $\text{LaFeAsO}_{0.9}\text{F}_{0.1}$ . Interestingly, the large magnitudes of SHC  $\sim 1300\hbar e^{-1}\Omega^{-1}\text{cm}^{-1}$  in  $\text{KFe}_2\text{As}_2$  with a residual resistivity of  $\sim 10\mu\Omega\text{cm}$  is comparable to that ( $\sim 1000\hbar e^{-1}\Omega^{-1}\text{cm}^{-1}$ ) predicted for Pt with a substantially larger SOC in the same metallic regime, where the observed SHC  $\sim 240\hbar e^{-1}\Omega^{-1}\text{cm}^{-1}$  is reproduced at higher resistivity  $\sim 100\mu\Omega\text{cm}$  [7, 10, 11]. We shall trace the origin of the large SHC in  $\text{KFe}_2\text{As}_2$  in a special band feature later.

Since the SHE is found to be significantly affected by the doping level, we next investigate the effect of carrier doping by systematically varying the band filling over a range ( $n = 5.5 - 6.5$ ) that goes from electron doped ( $n > 6$ ) to hole doped ( $n < 6$ ) sides as relevant to the family of these materials. To single out the effect of doping we adopt a rigid-band calculation using the band structure of  $\text{BaFe}_2\text{As}_2$  that is known to cover both electron doping as in  $\text{Ba}(\text{Fe}_{1-x}\text{Co}_x)_2\text{As}_2$  and hole doping as in  $\text{Ba}_{1-x}\text{K}_x\text{Fe}_2\text{As}_2$ . Here we only consider the Fermi-surface part, which is found to be dominant as discussed above. The result, a curve in Fig. 2, exhibits a

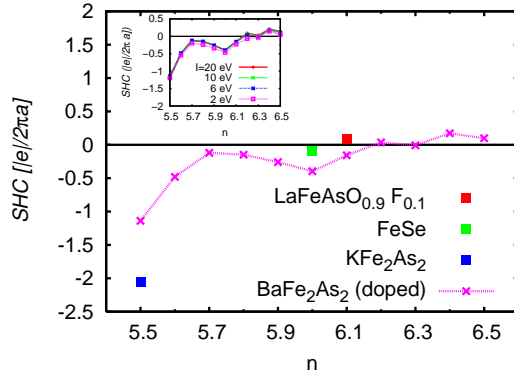


FIG. 2: Results for the spin Hall conductivity for various systems (symbols). The curve is the doping dependence in the rigid-band approximation for the band structure of BaFe<sub>2</sub>As<sub>2</sub>. Inset shows the dependence of the result on the strength of impurity potential.

large SHC in the heavily hole-doped regime ( $n \simeq 5.5$ ), while the magnitude is small in the weakly hole-doped and electron-doped regimes. The overall filling dependence agrees with the results for KFe<sub>2</sub>As<sub>2</sub> ( $n = 5.5$ ), FeSe ( $n = 6.0$ ), and LaFeO<sub>0.9</sub>F<sub>0.1</sub> ( $n = 6.1$ ), and highlights the presence of a common feature. Small deviations from the rigid-band result should be due to deformations in the electronic structures, such as the stronger three dimensionality in BaFe<sub>2</sub>As<sub>2</sub>.

As for the dependence on the impurity potential strength, we have checked, as shown in the inset of Fig. 2, that, when we vary the strength over ( $I \sim 2 - 20$ ) eV, the SHC, including its filling dependence, is rather insensitive to the strength of impurity potential[32]. This hallmarks an intrinsic nature of SHE in these materials.

Let us now focus on the case of heavily hole-doped KFe<sub>2</sub>As<sub>2</sub> that exhibits the large SHC. In order to identify its origin we explore if certain special band features around the Fermi energy are responsible. For this purpose we look into the momentum-dependent contribution of electronic states on the Fermi surface to the dominating Fermi-surface part in SHC,  $\sigma_{xy}^{z1}(\mathbf{k}) = \frac{1}{8} \sum_{k'=\pm k_x, \pm k_y, \pm k_z} \text{Tr}[(\hat{J}_x^S \hat{G}^R \hat{J}_y^C \hat{G}^A - \hat{J}_y^S \hat{G}^R \hat{J}_x^C \hat{G}^A)/2]_{k', \omega=0}$  where we are averaging over  $xy$  and  $yx$  components etc, with  $\frac{1}{2\pi N} \sum_{\mathbf{k}} \sigma_{xy}^{z1}(\mathbf{k})$  providing the net contribution of the Fermi surface part  $\sigma_{xy}^{z1}[7]$ .

We have only to consider a part of the Brillouin zone, as shown by the dotted area in Fig. 3 (a), while the other parts can be deduced from the symmetry. For clarity we consider the  $k_z = \pi$  plane, as other planes give qualitatively similar contributions due to quasi-2D nature of the Fermi surface that is also apparent from the almost flat dispersion near the Fermi level along  $\Gamma - T$  direction (Fig. 1). Figure 3 (b) shows that a huge contribution to SHC comes from a small region on the hole pocket near P. On the other hand, contributions from the rest of the Fermi surface are not only small but

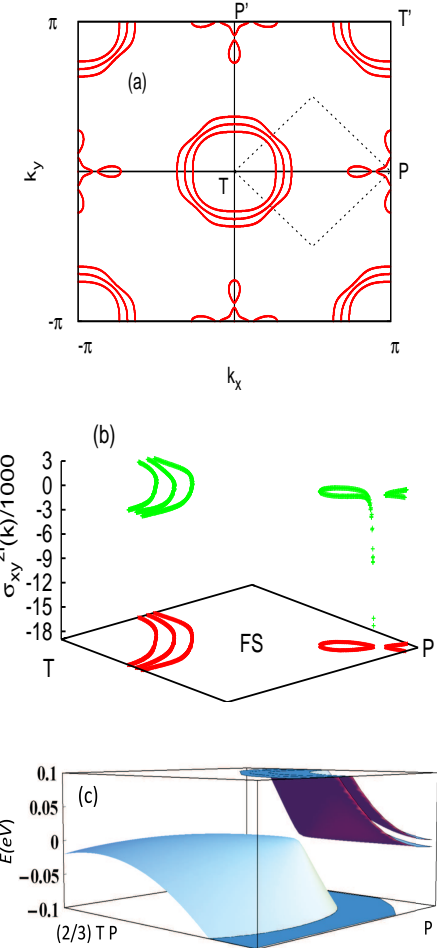


FIG. 3: (a) Fermi surface for KFe<sub>2</sub>As<sub>2</sub> shown on the  $k_z = \pi$  plane. (b)  $\mathbf{k}$ -dependent contribution from the states on the Fermi surface (red lines) to SHC (green), displayed for a part of Fermi surface (dotted region in (a)). Contribution from the other parts of the Fermi surface can be deduced from the symmetry. (c) Gapped Dirac cone dispersion near P. Electronic states make the huge contribution to SHC (b) in the close vicinity of the gap.

also tend to cancel with each other. Therefore, origin of the large SHC can be attributed to the huge contribution of electronic states on the hole pocket near P.

We can actually identify, in Figures 3 (c) and 4, that these electronic states lie in the close vicinity of a small SOC-induced gap in the Dirac cone, which is tilted. This is also the case with our analysis for the filling dependence in BaFe<sub>2</sub>As<sub>2</sub> with a rigid band, where we find a similar origin behind the large SHC in the heavily hole-doped regime ( $n \simeq 5.5$ ), in which the Fermi level approaches the Dirac point. Concomitantly, such Dirac-like points near the Fermi level are absent in FeSe and LaFeAsO<sub>0.9</sub>F<sub>0.1</sub>. Such Dirac-like points arise due to crossing of two bands that respectively have almost linear dispersions and different orbital characters as a consequence of crystal symmetries in the iron-based mate-

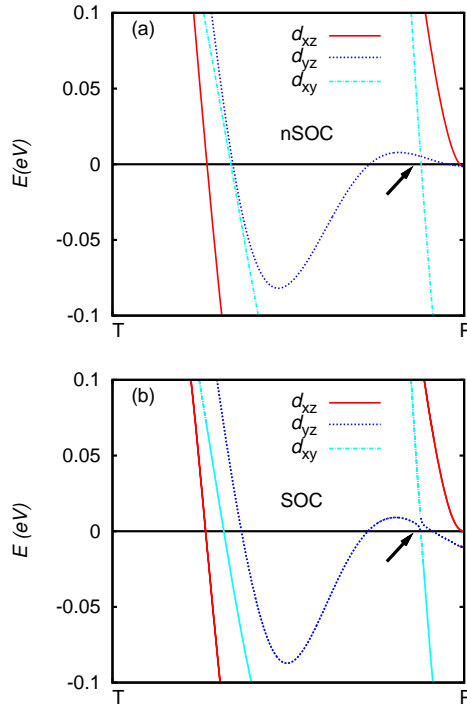


FIG. 4: The band dispersions for the electronic states in KFe<sub>2</sub>As<sub>2</sub> without SOC (a) and with SOC (b). The Dirac point, around which dominant contributions to SHC arise as shown in Fig. 3, is indicated with arrows.

rials, as also discussed recently in detail by Anderson and Boeri[20]. In the present case, as shown in Fig. 4, while one of the crossing bands has dominantly *yz* orbital character, the other band has *xy* character. The band crossing is a consequence of the opposite parities of the two orbitals with respect to reflection to *xz* mirror plane. In the presence of an SOI, the gap opens at the Dirac point because the two orbitals are then coupled by the *y*-component of the orbital angular momentum  $\hat{l}_y$ ;  $\langle yz | \hat{l}_y | xy \rangle = -i$ .

Thus the large SHC when the Fermi level lies close to the SOC-induced gap at the Dirac point renders the iron-based systems a Dirac electron systems, as in graphene.[21] The difference here is, unlike in graphene, the gap can be large enough to make the SHE experimentally accessible due to relatively strong strength of SOC for 3d electrons. We briefly comment on the role of current vertex corrections due to local impurity potentials. In the present investigation, as we consider only Fe 3d electrons, they vanish identically as a consequence of the even parity of *d*-electrons with respect to  $\mathbf{k} \rightarrow -\mathbf{k}$  [10]. However, in the presence of *p* electrons with an odd parity that come from the other elements such as pnictogens and chalcogens, the current vertex corrections may be finite, as indeed found in graphene[33]. Nevertheless, we expect that the present result would not be modified significantly as the dominant contribution to electronic states around the Fermi level comes from the Fe 3d or-

bitals.

In summary, we have theoretically explored the possibility of spin Hall effect in a variety of the recently discovered iron-based superconducting materials. We reveal that a substantially large spin Hall current arises in heavily hole-doped systems such as KFe<sub>2</sub>As<sub>2</sub>, whose magnitude is comparable with that in Pt. The large spin Hall current is found to come from a huge contributions from the electronic states in the vicinity of the spin-orbit coupling induced gap at the Dirac points that is made to lie close to the Fermi level in the heavily doped case.

S. P. is supported by the JSPS Postdoctoral Fellowship for Foreign Researchers, Japan. R. A. is supported by the JST PRESTO program, Japan.

---

[1] For a recent review, see, e.g., G. Vignale, *J. Supercond. Nov. Magn.*, **23**, 3 (2010).

[2] J. E. Hirsch, *Phys. Rev. Lett.* **83**, 1834 (1999).

[3] M. I. D'yakonov, and V. I. Perel', *Sov. Phys. JETP Lett.* **13**, 467 (1971); *ibid. Phys. Lett. A* **35**, 459 (1971).

[4] Y. Kato *et al.*, *Science* **306**, 1910 (2004).

[5] T. Kimura *et al.*, *Phys. Rev. Lett.* **98**, 156601 (2007).

[6] L. Vila *et al.*, *Phys. Rev. Lett.* **99**, 226604 (2007).

[7] H. Kontani *et al.*, *J. Phys. Soc. Jpn.* **76**, 103702 (2007).

[8] G. Y. Guo *et al.*, *Phys. Rev. Lett.* **100**, 096401 (2008).

[9] H. Kontani *et al.*, *Phys. Rev. Lett.* **100**, 096601 (2008).

[10] T. Tanaka *et al.*, *Phys. Rev. B* **77**, 165117 (2008).

[11] H. Kontani *et al.*, *Phys. Rev. Lett.* **102**, 016601 (2009).

[12] G. Y. Guo *et al.*, *Phys. Rev. Lett.* **102**, 036401 (2009).

[13] B. Gu *et al.*, *Phys. Rev. Lett.* **105**, 086401 (2010).

[14] T. Tanaka and H. Kontani, *Phys. Rev. B* **81**, 224401 (2010).

[15] F. Freimuth *et al.*, *Phys. Rev. Lett.* **105**, 246602 (2010).

[16] M. Morota *et al.*, *Phys. Rev. B* **83**, 174405 (2011).

[17] A. Fert and P. M. Levy, *Phys. Rev. Lett.* **106**, 157208 (2011).

[18] For a recent review, see e.g. F. Wang *et al.*, *Science* **332**, 200 (2011).

[19] K. Kuroki *et al.*, *Phys. Rev. Lett.* **101**, 087004 (2008); *ibid* **102**, 109902(E) (2009); *Phys. Rev. B* **79**, 224511 (2009).

[20] O. K. Anderson and L. Boeri, *Annalen der Physik*, **1**, 8 (2011).

[21] C. L. Kane and E. J. Mele, *Phys. Rev. Lett.* **95**, 146802 (2005).

[22] Y. Yao *et al.*, *Phys. Rev. B* **75**, 041401 (2007).

[23] T. Naito *et al.*, *Phys. Rev. B* **81**, 195111 (2010).

[24] M. Z. Hasan and C. L. Kane, *Rev. Mod. Phys.* **82**, 3045 (2010).

[25] J. P. Perdew *et al.*, *Phys. Rev. Lett.* **77**, 3865 (1996).

[26] P. Blaha *et al.*, <http://www.wien2k.at/>

[27] J. Kunes *et al.*, *Phys. Rev. B* **64**, 153102 (2001).

[28] J. Kunes *et al.*, *Comput. Phys. Commun.* **181**, 1888 (2010).

[29] A. A. Mostofi *et al.*, *Comput. Phys. Commun.* **178**, 685 (2008).

[30] As for the full minimization of the size of the Wannier functions, see N. Marzari *et al.*, *Phys. Rev. B* **56**, 12847

(1997); I. Souza *et al.*, *ibid.* **65**, 035109 (2001).

[31] P. Streda, J. Phys. C **15** L717 (1982).

[32] K. Nakamura, R. Arita, and H. Ikeda, Phys. Rev. B **83**, 144512 (2011), have estimated the impurity potential strengths for various elements, which lie around  $|I| \sim < 8$  eV.

[33] S. Onari *et al.*, Phys. Rev. B **78**, 121403 (2008).